Tunnelling and Underground Space Technology 81 (2018) 55–67

Contents lists available at ScienceDirect

Tunnelling and Underground Space Technology

journal homepage: www.elsevier.com/locate/tust

# Discrete element modelling of stress-induced instability of directional drilling boreholes in anisotropic rock

Kang Duan[a], Wei Wu[a,*], Chung Yee Kwok[b,*]

[a] School of Civil and Environmental Engineering, Nanyang Technological University, Singapore
[b] Department of Civil Engineering, The University of Hong Kong, Hong Kong, China

ARTICLE INFO

*Keywords:*
Discrete element method
Borehole instability
Directional drilling
Anisotropic rock

ABSTRACT

Directional drilling is a viable and cost-effective trenchless technology for the installation of pipelines and conduits in shallow formations and the extraction of unconventional energy resources in deep reservoirs. The performance of drilled boreholes is associated not only with drilling practice (e.g., borehole size and drilling direction) but also with geological environment (e.g., in-situ stress and geomaterial property). We conduct discrete element modelling on hollow anisotropic rock samples to elucidate the stress-induced instability along a directional drilling borehole with vertical, inclined, and horizontal sections. We systematically evaluate the influences of confining pressure, borehole diameter, and bedding orientation on the mechanical response of the hollow samples. When the confining pressure increases, the peak stress varies from a linearly increasing fashion for relatively small borehole diameters to an unstable variation trend for relatively large borehole diameters. Both peak stress and elastic modulus decrease with larger borehole diameter. The effects of bedding planes are negligible when the borehole exists perpendicular to bedding planes, while borehole instability likely occur when the borehole is oriented along bedding planes. The presence of bedding planes leads to the concentration of tangential stress along the normal direction of bedding planes, which ultimately dominates the failure mechanisms at the particle scale. With the increase of anisotropy angle, the dominant failure modes transform from the tensile failure of rock matrix to the shear failure along bedding planes.

## 1. Introduction

Advances in trenchless technologies, like microtunneling and horizontal directional drilling, have enabled the rapid development of underground infrastructure installation (e.g., pipelines and conduits) and unconventional energy extraction (e.g., natural gas and geothermal energy). The efficiency of the invisible and quiet excavation relies on our deep understanding of the mechanical response of disturbed geomaterials around boreholes. For example, drilling fluids significantly influence borehole stability in loose sand (Wang and Sterling, 2007) and fractured rock (Shu and Zhang, 2018) at shallow depths. In deep directional drilling, rock anisotropy is one of the most distinct features influencing borehole stability in sedimentary formations. The directional drilling may start from isotropic rock (e.g., sandstone and limestone) at shallow layers, and subsequently extend into energy-bearing anisotropic rock (e.g., shale and coal) at great depths. Fig. 1 shows a directional drilling borehole composed of the vertical, inclined, and horizontal sections. The borehole instability in different sections is associated not only with rock fabric controlling the magnitude and orientation of in-situ stress, but also stress redistribution causing the stress-dependent anisotropy (Amadei, 1996). Both rock fabric and redistributed stress lead stress-induced borehole instability to be one of the major challenges of drilling highly inclined wells in anisotropic rock (Okland and Cook, 1998). Several factors have been identified to influence the borehole instability, e.g., borehole size (Dresen et al., 2010), drilling orientation (Meier et al., 2014), and in-situ stress (Haimson and Chang, 2002; Zheng et al., 1989). However, our understanding of stress-induced borehole instability is still limited due to the complicated process of crack development under the combined effects of bedding orientation and in-situ stress states.

Numerous attempts have been made to explore the mechanism of stress-induced borehole instability. In experimental studies, a series of laboratory tests at reduced scales have been conducted to elucidate the mechanism of either stress-induced (Meier et al., 2013) or drilling-induced borehole breakouts (Haimson and Lee, 2004). Several aspects of the borehole instability problem have been investigated, including the influences of bedding angle (Meier et al., 2014), borehole diameter (Meier et al., 2013), stress anisotropy (Haimson and Lee, 2004), and

---

* Corresponding authors.
*E-mail addresses:* wu.wei@ntu.edu.sg (W. Wu), fkwok8@hku.hk (C.Y. Kwok).

https://doi.org/10.1016/j.tust.2018.07.001
Received 25 January 2018; Received in revised form 25 May 2018; Accepted 3 July 2018

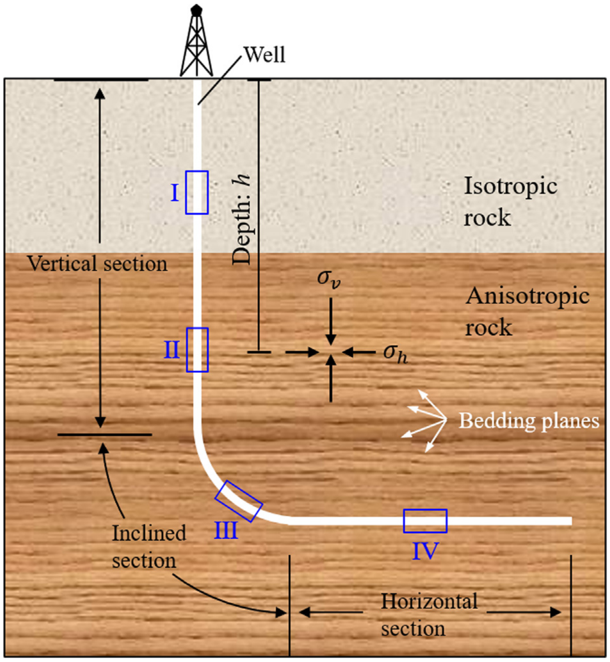

**Fig. 1.** A complete borehole with vertical section in isotropic rock (Section I) as well as vertical (Section II), inclined (Section III), and horizontal (Section IV) sections in anisotropic rock.

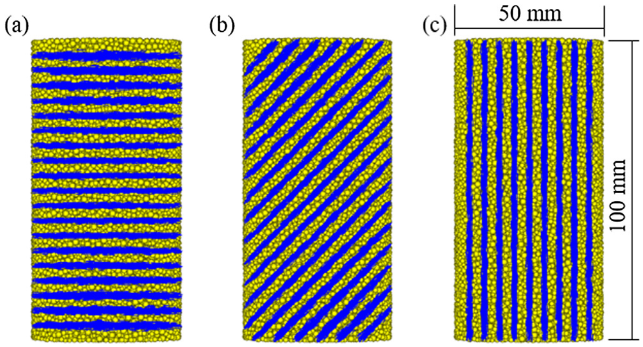

**Fig. 2.** DEM models with varying anisotropy angles: (a) $\beta = 0^\circ$, (b) $\beta = 45^\circ$, and (c) $\beta = 90^\circ$. Yellow balls represent rock matrix, and blue discs act as smooth-joint contacts inserted to represent bedding planes. (For interpretation of the references to colour in this figure legend, the reader is referred to the web version of this article.)

**Table 1**
Micro-parameters calibrated for the DEM model to represent the Posidonia shale.

| Particle parameters | | Parallel bond parameters | | Smooth joint parameters | |
|---|---|---|---|---|---|
| $E_c$ (GPa) | 17.5 | $\bar{E}_c$ (GPa) | 17.5 | $\bar{k}^n$ (GPa/m) | 1630 |
| $k_n/k_s$ | 1.45 | $\bar{k}_n/\bar{k}_s$ | 1.45 | $\bar{k}^s$ (GPa/m) | 1000 |
| $\mu$ | 0.5 | $\bar{\sigma}_c$ (MPa) | 107±24 | $\sigma_c$ (MPa) | 5 |
| $R_{max}/R_{min}$ | 1.66 | $\bar{\tau}_c$ (MPa) | 107±24 | $c_b$ (MPa) | 13 |
| $R_{min}$ (mm) | 0.75 | $\bar{\lambda}$ | 1.0 | $\varphi$ (Â°) | 30 |
| $\rho$ (kg/m$^3$) | 3700 | | | $\mu_c$ | 0.5 |

$E_c$, the contact modulus; $\bar{E}_c$, the parallel bond modulus; $k_n/k_s$, the contact stiffness ratio (normal/shear); $\bar{k}^n/\bar{k}^s$, the parallel bond stiffness ratio (normal/shear); $\bar{\lambda}$, the parallel bond radius ratio; $\mu$, the coefficient of friction; $\rho$, density of particle; $\bar{\sigma}_c$ and $\bar{\tau}_c$, tensile and shear strength of parallel bond; $R_{\max}$ and $R_{\min}$, the maximum and minimum radius of particles. $\bar{k}^n$ and $\bar{k}^s$, the normal and shear stiffness of smooth joint; $\sigma_c$, the tensile strength; $c_b$ and $\varphi$, the cohesion and friction angle; $\mu_c$, the friction of coefficient of the smooth joint.

**Table 2**
Comparison between the mechanical properties obtained from our DEM simulation and the mechanical properties of the Posidonia shale under uniaxial compression (Meier et al., 2014).

| | $\beta$ (°) | Uniaxial compression strength (MPa) | | Young's modulus (GPa) | |
|---|---|---|---|---|---|
| | | Experiments | DEM | Experiments | DEM |
| Anisotropic model | 0 | 115 ± 7 | 114.4 | 10.4 | 10.1 |
| | 45 | 60 ± 10 | 62.9 | – | 11.0 |
| | 90 | 75 ± 7 | 81.4 | 17.3 | 17.1 |
| Isotropic model | – | – | 121.98 | – | 20.86 |

time-dependent behavior (Kupferschmied et al., 2015). In these studies, the patterns of borehole instability are always imaged after the tests. However, it is difficult to directly observe the evolution of micro-features during the tests, which leads to a lack of thorough observation of underlying failure mechanism. Moreover, most of the tests are conducted on hollow cylindrical samples following hydrostatic loading paths (Ewy and Cook, 1990; Zoback et al., 1985). In such cases, when a borehole is along the maximum principal stress, the influence of axial stress is usually overlooked due to the assumption of plane strain problem.

The numerical and analytical analyses of stress-induced borehole instability have also been developed in two aspects: calculation of stress distribution around a borehole, and estimation of fracture pattern with the stress-related failure criteria (Al-Ajmi and Zimmerman, 2006; Gaede et al., 2012). The assumptions of linear elastic and isotropic materials have been most commonly adopted together with the linear failure criterion. However, rock formations might be anisotropic with respect to both deformability and strength. Although the analytical solution for stress distribution around a borehole in anisotropic formations is available (Amadei et al., 1983), the stress redistribution after the occurrence of borehole instability is a dynamic process and difficult to be described by continuum modeling.

The development of discontinuum model offers great promise to study the initiation and propagation of induced fractures and their interaction with pre-existing discontinuities (e.g., bedding planes), due to its explicit representation of rock discontinuities (Duan et al., 2018; Zhao et al., 2011). The DEM (discrete element method) modeling of anisotropic rock has been developed by inserting either continuous (Lisjak et al., 2015) or discontinuous bedding planes (Duan et al., 2016). For the borehole instability analyses, the DEM simulation has been performed to investigate the evolution of borehole breakouts (Duan and Kwok, 2016) and the formation of shear fractures (Lee et al., 2015). Most of these studies are conducted in two-dimensions, which neglects the influence of axial stress. The simulation on three-dimensional models is necessary since triaxial stress states have been proven to play an important role in the mechanical properties of rocks (Haimson and Chang, 2002; Ma and Haimson, 2016).

In this study, we performed DEM modelling on hollow anisotropic rock samples to investigate the mechanism of boreholes instability. The effects of confining pressure, borehole diameter, and bedding orientation were systematically evaluated by examining the stress-strain curve, peak stress, and elastic modulus. All these simulations were conducted based on the three-dimensional particle flow code (PFC3D) (Itasca, 2008).

## 2. Numerical models

### 2.1. Genesis of the intact anisotropic model

In the DEM model, the rock matrix is represented as an assembly of rigid particles bonded at their contacts, which is known as the bonded